Eradication of CD19 + Leukemia by Targeted Calicheamicin θ

ARTICLE *in* BIOCONJUGATE CHEMISTRY · AUGUST 2009

Impact Factor: 4.51 · DOI: 10.1021/bc900128h · Source: PubMed

6 AUTHORS, INCLUDING:

Nicole Huebener
Charité Universitätsmedizin Berlin
39 PUBLICATIONS **404** CITATIONS
SEE PROFILE

Gerhard Gaedicke
Medizinische Universität Innsbruck
215 PUBLICATIONS **3,026** CITATIONS
SEE PROFILE

Holger N Lode
University of Greifswald
156 PUBLICATIONS **2,816** CITATIONS
SEE PROFILE

Eradication of CD19$^+$ Leukemia by Targeted Calicheamicin θ

Kathrin M. Bernt,[‡] Aram Prokop,[§] Nicole Huebener,[‡] Gerhard Gaedicke,[†,‡] Wolfgang Wrasidlo,[†,||] and Holger N. Lode*[,‡]

Charité Universitätsmedizin Berlin, Department of Pediatrics, Experimental Oncology, Berlin, Germany, Department of Pediatric Hematology/Oncology, Berlin, Germany, and Moore's Cancer Center, University of California, San Diego, California. Received March 24, 2009; Revised Manuscript Received May 18, 2009

Children with relapsed and refractory acute lymphoblastic leukemia (ALL) still face a critical prognosis. We tested the hypothesis that targeted calicheamicin theta (θ) using an anti-CD19-immunoconjugate may provide an effective treatment strategy for CD19$^+$ ALL. Calicheamicin θ is a rationally designed prodrug of the natural enediyene calicheamicin γ, obtained by total synthesis. It offers the advantage of increased in vivo stability and 1000-fold higher antitumor potency over calicheamicin γ. First, we demonstrate efficacy of calicheamicin θ against primary pre-B leukemic cells and multidrug-resistant leukemia cell lines ($IC_{50} = 10^{-9}$ to 10^{-12} M). Second, conjugation of calicheamicin θ to an internalizing murine anti-CD19 monoclonal antibody was demonstrated to affect neither calicheamicin θ mediated cytotoxicity nor binding of the antibody to the target molecule. Third, anti-CD19-calicheamicin θ immunoconjugate revealed a maximum tolerated dose of 10 μg/kg and CD19-specific and long-lasting eradication of established leukemia was demonstrated in a xenograft model. Finally, we show that the antileukemic effect of anti-CD19-calicheamicin θ is mediated by induction of apoptosis proceeding through the caspase-mediated mitochondrial pathway. On the basis of these results, we conclude that anti-CD19-calicheamicin θ immunoconjugates may offer a novel and effective approach for the treatment of relapsed CD19$^+$ ALL.

INTRODUCTION

The treatment success of pediatric patients with newly diagnosed acute lymphoblastic leukemia (ALL) has dramatically inproved over the last decades and overall cure rates are above 70% (*1, 2*). However, one of the limitations remains a relapse rate of nearly 30% (*3*) as described in stratified and randomized multicenter trials such as ALL-REZ BFM 85 (*4*). Although the overall second complete remission (CR) rate was 92%, the probability of event-free survival (EFS) at 6 years was only 0.31 ± 0.04. Thus, the proposed treatment regimen can induce long-lasting second remissions in about one-third of patients even after intensive front-line treatment. However, the majority of patients still face a critical prognosis particularly subsequent to early relapse.

Alternative treatment approaches to B-cell malignancies were established by using a monoclonal antibody directed against the common B-cell differentiation antigen CD20. Efficacy of adjuvant immunotherapy using anti-CD20 in low-grade B-cell lymphoma has been clearly demonstrated (*5, 6*) suggesting that anti-CD20 therapy is also effective in more aggressive, high-grade B-cell malignancies such as Burkitts and diffuse large-cell lymphoma (*7*−*10*). The mechanism of action mediated by anti-CD20 is a combination of humoral and cellular immune responses (*11*) and the induction of apoptosis in cells targeted by the antibody (*12*), which can be further improved by labeling the antibody with radioisotopes (*13*). However, the use of this anti-CD20 antibodies in pediatric leukemias is limited by the fact that pre-B cell leukemias do not express CD20. This is in contrast to CD19, an earlier differentiation marker in B-cell differentiation. CD19 expression is induced at the point of B lineage commitment during the differentiation of the hematopoietic stem cell, and its expression continues through preB and mature B cell differentiation until it is finally down-regulated during terminal differentiation into plasma cells. CD19 expression is maintained in B-lineage cells that have undergone neoplastic transformation, and therefore, CD19 is a useful target in leukemia and lymphoma thearpy using monoclonal antibodies (*14, 15*). CD19 is highly expressed by the majority of relapsed ALL leukemic cells and immunotoxins targeted to CD19 were shown to mediate apoptosis also in rituximab-resistant hematologic malignancies (*16*).

Since induction of apoptosis is one important mechanism of action mediated by anti-CD19 antibodies (*14*), we intended to amplify the mode of action by fusing an anti-CD19 antibody to the enediyene calicheamicin θ. Enediyenes are a group of cytotoxic compounds identified from a broth extract of a soil microorganism, *Micromonospora echinospora calichensis*, which were termed calicheamicins. These compounds were later identified as members of a class of antibiotics incorporating the enediyne moiety which include the esperamicins, dynemicins, and neocarzinostatin (*17*) which were found to exert impressive potencies in a screen for DNA damaging agents (*18*) that exceeded the cytotoxic potency of substances such as CN-MRA (*19*) and ricin (*20*), which have been claimed as some of the most toxic substances known at the time. Within this group of enediyene antibiotics, calicheamicin γ was the most potent compound, which was found to bind in the minor groove of DNA, and the resulting sequence-specific DNA-cleavage has been described (*21*). A novel biologically active and selective enediyene molecule calicheamicin θ was rationally designed on the basis of the mechanism of action of the naturally occurring calicheamicin γ. Unlike its natural counterpart, calicheamicin θ contains structural variations that facilitate molecular triggering to form the active compound under mild

* Holger N. Lode, Charité Universitätsmedizin Berlin, Experimental Oncology, Forum 4, R 2.0407, Augustenburger Platz 1, 13353 Berlin, Germany, E-mail: holger.lode@charite.de. Tel.: + 49 30 450 566233, Fax: +49 30 450 566916.

[‡] Department of Pediatrics, Experimental Oncology.

[§] Department of Pediatric Hematology/Oncology.

[†] Charité Universitätsmedizin Berlin.

[||] University of California.

10.1021/bc900128h CCC: $40.75
Published on Web 07/02/2009

Table 1. Effect of Calicheamicin θ against Primary Patients ALL and Leukemia Cell Lines[a]

cell line[b]	cell type	calicheamicin θ IC_{50} [M][c]
Molt-3	T-cell	2.0×10^{-12}
Molt-4	T-cell	1.5×10^{-13}
MOVP-3	T-cell	4.5×10^{-11}
TCAF	T-cell	1.1×10^{-11}
HL60	Promyelocytic	3.6×10^{-11}
L1210	Lymphocytic Leukemia[d]	1.8×10^{-10}
P-388	Lymphocytic Leukemia[d]	4.5×10^{-9}
Nalm-6	pre B-cell	9.0×10^{-13}
Reh	pre B-cell	1.5×10^{-12}
Patient I	ALL	4.8×10^{-12}
Patient II	ALL	1.9×10^{-10}
Patient III	ALL	5.2×10^{-10}

[a] The IC_{50} concentration of calicheamicin θ was determined against ALL blasts and leukemia cell lines using the XTT assay. [b] Cells used for calicheamicin θ drug sensitivity testing were human and murine cell lines. [c] Values represent the means of experiments in triplicate. Standard deviations were below 10%. [d] Cells of murine origin.

Table 2. Cytotoxicity of Chemotherapeutic Agents on NALM-6 Cells

drug[a]	target	IC_{50} [M][b]
Calicheamicin θ	DNA minor groove (TCCT)	5×10^{-13}
Doxorubicin	topoisomerase II	3×10^{-10}
Camptothecan	topoisomerase I	4×10^{-9}
Paclitaxel	tubulin, microtubles	1×10^{-10}
Etoposide	topoisomerase II	1×10^{-8}
Melphalan	alkylation of DNA	4×10^{-8}
Methotrexate	dihydrofolate reductase	6×10^{-8}
Vinblastine	microtuble depolymerization	2×10^{-6}
Genistein	Src kinase family blocker	6×10^{-6}
Calicheamicin θ -anti CD19	CD19	2×10^{-13}
Doxo-anti-CD19	CD19	1×10^{-9}
Doxo-anti-CD20	CD20	3×10^{-9}
Doxo-anti-CD22	CD22	8×10^{-10}
AntiCD19, 20, 22	CD19, CD20, CD22	$>1 \times 10^{-4}$
Calicheamicin θ -anti CD19[c]	$CD19^+$ (NALM-6)	5×10^{-11}
Calicheamicin θ -anti CD19[c]	$CD19^-$ (Molt-3)	6×10^{-8}

[a] The IC_{50} concentration of indicated chemotherapeutic agents was determined against NALM-6 B-cell lymphoblastic leukemia using the XTT assay. [b] Values represent the means of experiments in triplicate. Standard deviations were below 10%. [c] The IC_{50} concentration of Calicheamicin θ -anti CD19 immunotoxin was determined in CD19 positive and negative cells using a short exposure experiments as described in Materials and Methods.

basic conditions (*22, 23*). This modification led to a further increase in cytotoxicity over the natural compound when tested against a large number of different human cancer cell lines as determined by the decrease in the concentration at which 50% of cell viability was observed (*22, 23*). The small size of calicheamicins with molecular weights of approximately 1500 Da combined with their unique mode of action and the extreme potency of calicheamicin θ suggest that this compound might be a good candidate for targeted chemotherapy. In fact, we demonstrated the use of calicheamicin θ for targeted therapy of neuroblastoma using antiganglioside GD2 antibodies (*24*). Here, we expand these findings and establish for the first time efficacy and mechanism of an antibody drug conjugate between a murine monoclonal anti-CD19 mAb and calicheamicin θ that suppresses growth and dissemination of leukemic cells in a Nalm-6 pre B-cell leukemia model.

MATERIALS AND METHODS

Cell Lines and Patient Cells. NALM-6, Reh, Molt-3, Molt-4, TCAF, TCAF-Dox, HL60, L1210, and P-388 cell lines were purchased from ATCC. Cells were maintained in RPMI with 10% fetal bovine serum. Control vector and FADD-dn-transfected BJAB cells expressing a dominant negative FADD mutant lacking the N-terminal death receptor domain have been described earlier (*25*). Leukemic cells from patients were isolated from bone marrow samples at initial diagnosis. Mononuclear cells were prepared by Ficoll centrifugation and characterized by flow cytometry. Patient cells were maintained in RPMI with 20% fetal bovine serum and gentamicin (50 μg/mL).

Mice. Female FOX CHASE C.B-17/lcrCrl-scid BR mice were obtained at 8 weeks of age from Charles River Laboratories, Sulzfeld, Germany. They were housed in the pathogen-free mouse colony at our institution in groups of 8 mice. Mice were fed ad libitum on standard mouse laboratory chow. Animal experiments were performed according to the German guide for the care and use of laboratory animals, i.e., "Tierschutzgesetz".

Cytostatic Agents, Antibodies, and Reagents. Anti-CD19 (mouse IgG2a) was obtained from CellGenics (Freiburg, Germany) and anti-CD19 (mouse IgG2b, clone HID-9703) and anti-CD20 (mouse IgG1, clone L-27) from Baxter (Unterschleissheim, Germany). Human-mouse chimeric antiganglioside GD2 antibody ch14.18 (*26*) was used as a negative control. Conjugation of mAbs with fluorescein isothiocyanate (FITC) was accomplished at pH 9.0 using 20 μL FITC solution (5 mg/mL in DMSO) per mg mAb (1 mg/mL). After 2 h, the pH was lowered to pH 7.4 and FITC-labeled antibody was purified over PD-10 columns (Amersham-Pharmacia, Freiburg, Germany).

Calicheamicin θ (MW 1464 g/mol) was obtained by total synthesis as previously described (*23*). Succinimidyl 6-(3-[2-pyridyldithio]-propionamido)hexanoate (LC-SPDP) and iminothiolane were obtained from PIERCE (Rockford, IL). Doxorubicin, camptothecan, paclitaxel, etoposide, melphalan, methotrexate, vinblastine, genistein, 2,3-bis(2-methoxy-4-nitro-5-sulfophenyl)-5-[(phenylamino)carbonyl]-2*H*-tetrazolium hydroxide (XTT), organic solvents, and phenazine methosulfate (PMS) were obtained from Sigma-Aldrich (Deisenhofen, Germany). All cytotoxic agents were dissolved in DMSO or DMF, and 10 mM stock solutions were stored at −20 °C until use. Cell culture reagents, restriction enzymes, and other molecular biology reagents were from Life Technologies (Karlsruhe, Germany).

Conjugation of Calicheamicin θ. The conjugation of calicheamicin θ to anti-CD19, anti-CD20, and anti-GD2 mAb involved the activation of the sugar amino groups with LC-SPDP, using 4-dimethylaminopyridine (DMAP, Aldrich, Munich, Germany) as a catalyst, followed by disulfide exchange with iminothiolane-modified anti-CD19 and anti-GD2 mAb. For activation, 1 mg calicheamicin θ (1 mg/mL in DMF) was reacted with a 2-fold molar excess of LC-SPDP (succinimidyl 6-(3-[2-pyridyldithio]-propionamido)hexanoate) (37 μL of 20 mM LC-SPDP in DMSO) at 4 °C for 6 h and stored in small aliquots at −80 °C until further use. Sulfhydryl groups were introduced in mAbs (2 mg in 2 mL PBS, pH 8.3) by adding 10 μL iminothiolane (4.4 mg dissolved in 1 mL DMF) for 1 h under nitrogen. The iminothiolane-modified antibody was purified by size exclusion chromatography using a NAP-5 column (Amersham-Pharmacia, Freiburg, Germany) preequilibrated with PBS. The conjugation of activated drugs with thiolated mAb was done at RT for 1 h under nitrogen, using a 5:1 molar ratio followed by size exclusion chromatography. Finally, solutions were filter sterilized. The purity was checked by HPLC analysis (G200 size exclusion column, PBS elution buffer, 0.5 mL/min flow). The number of drug molecules per mAb was on the average two, calculated from the absorption ratios at A333/A280 for calicheamicin in the HPLC spectrum. Free calicheamicin was not detectable in these preparations. The dosage of the conjugate for cytotoxicity experiments was calculated on the basis of the molar concentration of drug on the antibody.

CD19 Expression Analysis. For the analysis of CD19 expression on Nalm-6, Reh and Molt-3 (negative control) anti-CD19-FITC was used. Cells were blocked with PBS (0.1% BSA in PBS, pH 7.4) and incubated with anti-CD19-FITC (1 μg/10^6 cells) or a mouse IgG2a isotype control (PharMingen, La Jolla,

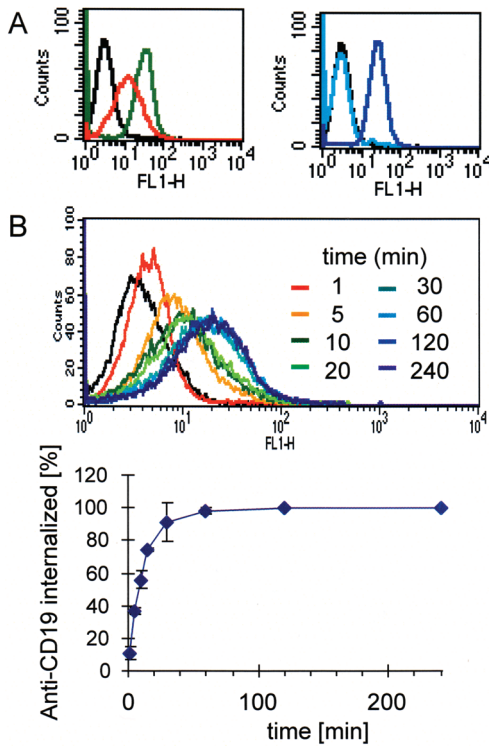

Figure 1. Internalization kinetics of anti-CD19 mAb. (A) Investigation of antibody internalization comparing two different anti-CD19 antibodies. Internalization of anti-CD19 (clone HID-9703) into Nalm-6 leukemia cells was demonstrated as indicated by an increase in fluorescence over background (red signal, left panel). Internalization was absent for anti-CD19 (IgG2a, Cell Genix) (light blue signal, right panel). Two control samples were incubated at 0 °C in the presence of 0.01% NaN_3 in order to block internalization. The first control sample (0 °C; 0.01% NaN_3) was stripped of bound antibody (black signals, left and right panels) and served as a negative control. The second control sample (0 °C; 0.01% NaN_3) was not stripped (green and dark blue signals, left and right panels) and was used as a positive control. All experiments were done in triplicate. (B) Internalization kinetics of anti-CD19 (clone HID-9703) into Nalm-6 leukemia cells over time. Mean fluoresence signals obtained from histograms (top) were used to calculate the percentage of internalized antibody (bottom). 100% equals the signal obtained with Nalm-6 cells incubated with anti-CD19-FITC antibody under non-internalizing conditions (0 °C in the presence of 0.01% NaN_3). Internalization (37 °C) was investigated over time by analysis of fluorescence signals resulting from internalization after stripping cells from non-internalized membrane-bound anti-CD19 antibody as described in Materials and Methods. Data represent mean ± sd ($n = 3$).

CA) for 20 min on ice, washed twice, and analyzed by FACScan (Becton Dickinson, Franklin Lakes NJ).

Internalization Assay of anti-CD-19-FITC. Cells were washed twice and blocked with PBS + 0.1% BSA on ice. Anti-CD19-FITC (1 μg/10^6 cells) was added on ice. Aliquots were subsequently transferred to 37 °C to allow for internalization. Negative control samples were incubated at 0 °C in the presence of 0.01% NaN_3, conditions which block internalization. An aliquot of each condition was retained at different time points to determine the total amount of bound and internalized antibody. At each time point, a second aliquot was stripped of noninternalized antibody with RPMI titered to pH 2.0 with HCl and adjusted to high salt (1 M NaCl, 2×, 15 min), and washed briefly in PBS (0.1% BSA, pH 7.4) before analysis. The quality of the stripping was assured by the total removal of all antibodies from control cells incubated under non-internalizing conditions. For the integration time course, experimental samples were incubated at 37 °C for the indicated time spans. The amount of integrated antibody in percent total integration was calculated as follows: MFI (time point)/MFI (4 h) × 100. The binding of calicheamicin conjugates was determined by indirect staining using a FITC-conjugated goat-anti mouse IgG secondary antibody (ParMingen), and secondary antibody only as control.

Cytotoxicity Assay. Cytotoxicity was determined by the XTT tetrazolium/formazan assay as previously described (*27*). Briefly, cells were seeded in 96 flat-bottomed well plates at a density of 10^4/well in 100 μL media, incubated overnight, and exposed to drug concentrations ranging from 10^{-6} to 10^{-16} M for calicheamicin θ or calicheamicin θ immunoconjugates and from 10^{-4} to 10^{-14} for all other drugs. In short exposure experiments, plates were washed (×2) by centrifugation after 1 h exposure to calicheamicin θ anti-CD19 immunoconjugates. Cell viability was assessed after 72 h by adding 50 μL XTT-reagent (1 mg/mL in RPMI) activated with 0.2% v/v PMS (1.53 mg/mL in PBS) incubated at 37 °C for 4 h. Plates were analyzed in a Thermomax (Molecular Devices) microplate reader at 450 nm. OD values were plotted as a function of drug concentration and the curves were integrated using the softmax software to obtain the IC_{50} concentration values. In experiments with BJAB cells, the cytotoxicity of calicheamicin θ immnunoconjugate was determined by the release of lactate dehydrogenase (LDH) using a detection kit from Boehringer-Mannheim (Mannheim, Germany).

Nalm-6 Xenograft Model. The Nalm-6 xenograft model was used as previously described (*28*). Briefly, leukemia was induced by injection of 1×10^6 Nalm-6 cells in 100 μL PBS (pH 7.4) into the tail vein of each SCID mouse. Mice ($n = 6$) were treated by intraperitoneal injection of PBS (pH 7.4), anti-CD19-calicheamicin θ and anti-GD2-calicheamicin θ immunoconjugates (1.0, 3.0, and 10.0 μg/kg linked calicheamicin θ; MW 1464 g/mol; 2 molecules per antibody) and anti-CD19 antibody (50, 150, and 500 μg/kg) (MW 150 000 g/mol) in a total volume of 200 μL. Each mouse received a total of 2 injections on days 5 and 7. Event-free survival of mice was followed over time. An event was defined by the development of central nervous system leukemia as indicated by presence paraplegia in individual mice.

Processing of Caspase 3, DNA Fragmentation, and Mitochondrial Permeability Transition. Processing of caspase 3, DNA fragmentation, and mitochondrial permeability transition was determined as previously described (*29*). Processing of caspase 3 was determined by Western blot using 30 μg of cytosolic protein probed with polyclonal rabbit antihuman caspase 3 antibody (1:2000). DNA fragmentation was investigated by flow cytometry of fixed cells after incubation with 50 μg/mL propidium iodide in PBS (pH 7.4), and data are expressed as percent of hypoploidy (subG1), reflecting the percentage of apoptotic cells. Mitochondrial permeability transition was analyzed by staining the cells with JC1 (Molecular Probes, Leiden, Netherlands). Determination of cells with decreased fluorescence signals consistent with mitochondria displaying a lower membrane potential was accomplished by flow cytometry. Data are expressed in percent of cells with low $\Delta\Psi_m$, which reflects the number of cells undergoing mitochondrial apoptosis.

Statistics. The statistical significance of differential findings between experimental groups of animals and control groups and between experimental and control samples was determined by two-tailed Student's *t* test. Findings were regarded as significant if two-tailed *p* values were <0.01.

RESULTS

Determination of the Efficacy of Calicheamicin θ against ALL Cells. The efficacy of calicheamicin θ against ALL cells was determined using a panel of cell lines and primary blasts from bone marrow of ALL patients (Table 1). The IC_{50} concentration for calicheamicin θ was in the picomolar range ($IC_{50} < 10^{-9}$ M) for the majority of ALL cells tested, including T-ALL and multidrug-resistant ALL, as well as the patients cells,

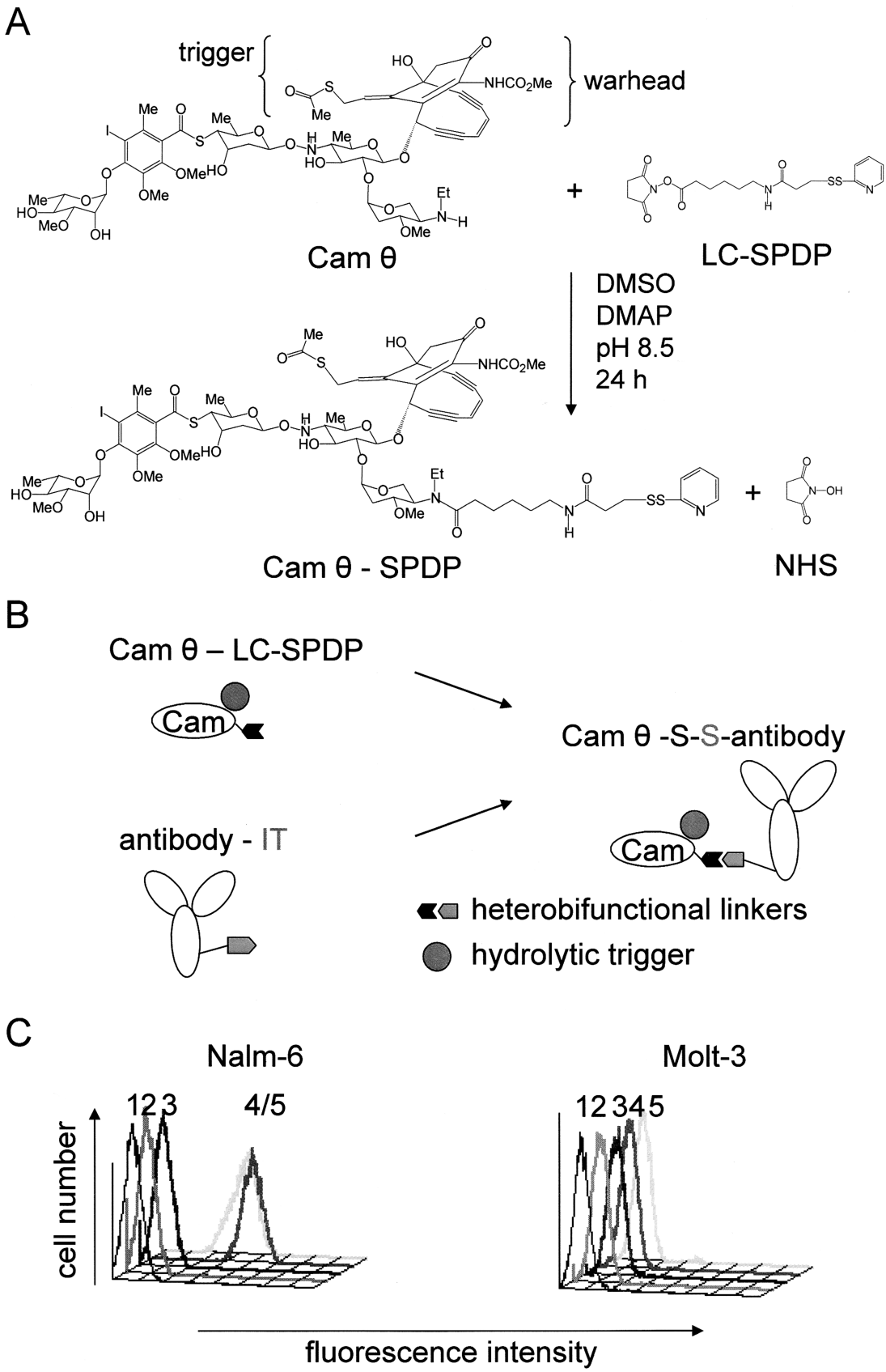

Figure 2. Synthesis and binding of anti-CD19 calicheamicin θ immunoconjugate. (A) Structures and reaction conditions of calicheamicin θ with the LC-SPDP linker to form calicheamicin θ-LC-SPDP. (B) Conjugation of calicheamicin θ-LC-SPDP with iminothiolane (IT) activated anti-CD19 (clone HID-9703) to form anti-CD19 calicheamicin θ immunotoxin. (C) Binding of anti-CD19 calicheamicin θ immunotoxin to CD19 positive Nalm-6 cells (left panel) in contrast to CD19-negative Molt-3 controls (right panel). 1, no antibody; 2, secondary antibody only; 3, anti-CD20; 4, anti-CD19; 5, anti-CD19 calicheamicin θ immunotoxin. All experiments were done in triplicate.

except for P-388 mouse lymphoblastic leukemia. In some cell lines (Molt-4, Nalm-6), the efficacy was even in the femtomolar range ($IC_{50} < 10^{-12}$ M). In order to further evaluate these results, we compared the efficacy of calicheamicin θ with other

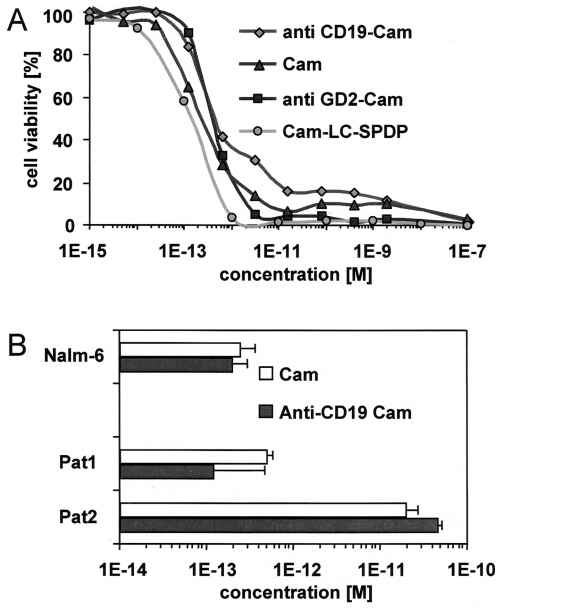

Figure 3. Cytotoxic effect of anti-CD19 calicheamicin θ immunoconjugate in vitro. A) The concentration dependent cytotoxic effects of calicheamicin θ, calicheamicin θ - LC-SPDP, anti-CD19 calicheamicin θ immunoconjugate and anti-GD2 calicheamicin θ immunoconjugate were determined on Nalm-6 cells. Data represent mean values of triplicate experiments. B) Cytotoxic effects of calicheamicin θ and anti-CD19 calicheamicin θ immunoconjugate against blasts obtained from relapsed ALL patients compared to Nalm-6 cells. Data represent IC50 concentrations (mean ± sd, $n = 3$).

established chemotherapeutic compounds used for ALL therapy on Nalm-6 cells (Table 2). Results revealed the lowest IC_{50} concentration for calicheamicin θ ($IC_{50} = 5 \times 10^{-13}$ M) in contrast to all other drugs tested, which were at best 1000-fold less active (i.e., doxorubicin $= 3 \times 10^{-10}$ M). These findings clearly demonstrate the excellent cytotoxic potential of calicheamicin θ for the generation of an immunotoxin for targeted therapy.

Generation and Characterization of an Anti-CD19 Calicheamicin θ Immunotoxin. The selection of the CD19 specific monoclonal antibody for the generation of a calicheamicin θ immunotoxin was based on antibody internalization experiments (Figure 1). Results indicate that the anti-CD19 antibody (Baxter) showed rapid internalization that was nearly complete after 60 min.

Therefore, this anti-CD19 antibody was selected for the conjugation to calicheamicin θ using the heterobifunctional linker LC-SPDP (Figure 2). The conjugation of the linker to calicheamicin θ is complicated by the highly unstable "trigger" and "warhead" portions of calicheamicin θ (Figure 2A). However, the conjugation of the activated NHS ester end of the LC-SPDP linker to the secondary amine of calicheamicin θ to form calicheamicin θ-LC-SPDP was accomplished in organic solvent at pH 8.5, without affecting the cytotoxic potential of calicheamicin θ (Figure 3). The 2-pyridylthiol group at the other end of the LC-SPDP linker was reacted with sulfhydryl residues in the anti-CD19 antibody to form a disulfide linkage (Figure 2B). Binding of the purified immunotoxin to CD19-positive Nalm-6 cells was demonstrated in contrast to CD19-negative Molt-3 cells used as negative controls (Figure 2C). The cytotoxic effect of anti-CD19-calicheamicin θ-immunotoxin was compared to that of free calicheamicin θ, calicheamicin θ-LC-SPDP and anti-GD2 calicheamicin θ (Figure 3A). Results indicate that the level of calicheamicin θ mediated cytotoxicity remained unchanged after conjugation to LC-SPDP and to a monoclonal antibody as determined in one ALL cell line and ALL blasts from bone marrow aspirates of two ALL patients (Figure 3B). We could also demonsrate an antigen-specific cytotoxic effect mediated by the anti-CD19-calicheamicin θ-immunotoxin in vitro since the IC_{50} on $CD19^-$ Molt 3 cells is 1000× higher than on $CD19^+$ Nalm-6 cells (Table 2). In summary, we could demonstrate that the conjugation affected neither antigen binding of the anti-CD19 portion of the immunotoxin nor the cytotoxicity of calicheamicin θ, resulting in an immunotoxin with antigen-specific cytotoxic potential similar to free calicheamicin θ.

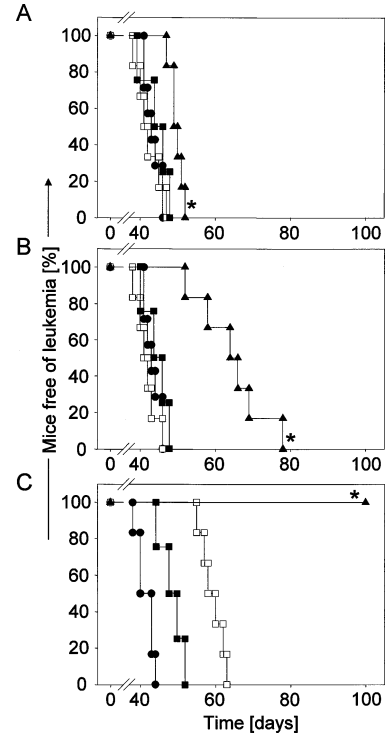

Figure 4. Effect of CD19 targeted calicheamicin θ in vivo. The effect of anti-CD19 calicheamicin θ immunotoxin against CD19-positive leukemia was determined in a xenograft model. Mice ($n = 6$ per group) were injected i.v. with 1×10^6 Nalm-6 cells. Treatment was initiated by two intraperitoneal injections on days 5 and 7 of 1.0 (A), 3.0 (B), and 10.0 μg/kg (C) with anti-CD19 calicheamicin θ immunotoxin (dose indicates linked calicheamicin θ) (closed triangle) and anti-GD2 calicheamicin θ immunotoxin control (open square). Controls received an equivalent amount of unconjugated anti-CD19 abtibody (500, 150, and 50 μg/kg) (closed square). Untreated control groups of animals received PBS injections (closed circles). Data represent the percentage of mice free of leukemia. The difference between groups of mice treated with anti-CD19 calicheamicin θ immunotoxin and all control groups was statistically significant (* $p < 0.01$).

Effect of Anti-CD19 Calicheamicin θ Immunotoxin in a Leukemia Xenograft Model. The efficacy of CD19-targeted calicheamicin θ therapy was evaluated in a leukemia xenograft model. For this purpose, CD19-positive Nalm-6 B-cell leukemia was established in SCID mice by intravenous injection (1×10^6 Nalm-6 cells). Treatment was initiated 5 days after tumor cell inoculation by two intraperitoneal injections of anti-CD19 calicheamicin θ immunotoxin per mouse (10, 3, and 1 μg/kg; dose indicates linked calicheamicin θ) on days 5 and 7. Controls received an equivalent amount of nonspecific anti-GD2 calicheamicin θ immunotoxin, unconjugated anti-CD19 antibody (500, 150, and 50 μg/kg), and PBS. A control group with free calicheamicin θ was not included, based on previous reports demonstrating high toxicity when used at an equivalent amount to 10 μg/kg calicheamicin θ immunotoxin (all animals died) and lack of activity when used at lower doses (*24, 30*). We selected the highest dose of 10 μg/kg calicheamicin θ immu-

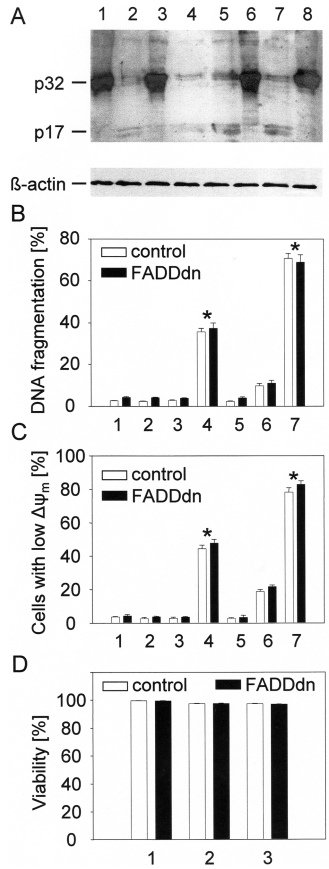

Figure 5. Apoptotic pathway induced by CD19 targeted calicheamicin θ. (A) The effect of anti-CD19 calicheamicin θ immunotoxin on processing of caspase 3 was determined in CD19-positive cALL lymphoblasts of a relapsed patient by Western blot. Procaspase 3 (p32) and activated caspase 3 fragment (p17) are indicated. 1, control (untreated); 2, anti-CD19 calicheamicin θ immunoconjugate (2 pmol/L); 3, anti-CD19 (2 pmol/L); 4, calicheamicin θ (2 pmol); 5, anti-CD19 calicheamicin θ immunoconjugate (20 pmol/L); 6, anti-CD19 (20 pmol/L); 7, calicheamicin θ (20 pmol/L); 8, control (untreated BJAB cells). Induction of DNA fragmentation after treatment for 72 h (B) and loss of mitochondrial membrane potential after treatment for 48 h (C) with anti-CD19 calicheamicin θ immunotoxin was investigated in CD19-positive BJAB cells in the presence (closed bars) and absence (open bars) of dominant negative FADD death receptor expression. 1, control; 2, anti-CD19 (1 pmol/L); 3, calicheamicin θ (1 pmol/L); 4, anti-CD19 calicheamicin θ immunotoxin (1 pmol/L); 5, anti-CD19 (10 pmol/L); 6, calicheamicin θ (10 pmol/L); 7, anti-CD19 calicheamicin θ immunotoxin (10 pmol/L). Data represent mean ± SD ($n = 3$). The difference between anti-CD19 calicheamicin θ immunotoxin and all controls was statistically significant (* $p < 0.01$). (D) Cytotoxic effects of calicheamicin θ immunotoxin were analyzed at concentrations levels with established proapoptotic effect. 1, control; anti-CD19 calicheamicin θ immunotoxin 2, 1 pmol/L; 3, 10 pmol/L. Data represent mean ± SD ($n = 3$).

notoxin based on previous reports demonstrating no toxicity at this level (*24*).

Treatment of mice ($n = 6$/group) with established CD19-positive leukemia using 10 μg/kg anti-CD19 calicheamicin θ immunotoxin (2×, days 5 and 7 after tumor cell inoculation) induced a 3-fold prolongation of the life span with all animals alive at the end of the experiment (Figure 4). Specificity of this therapy was demonstrated, since mice treated with an equivalent amount of anti-GD2 calicheamicin θ immunotoxin used as nonspecific control was far less effective at the 10 μg/kg dose and ineffective at the 3 and 1 μg/kg doses, respectively. Similarly, the use of unconjugated anti-CD19 antibody at dose levels of 3 and 1 μg/kg was ineffective. There was a small effect by unconjugated anti-CD19 antibody at the dose level of 10 μg/kg, related to antibody-mediated immunological effector functions. However, the anti-CD19 calicheamicin θ immunotoxin was far more effective. The treatment was well-tolerated, since none of the mice receiving 10, 3, and 1 μg/kg calicheamicin θ immunotoxin presented with a drop in body weight of >20% as shown by weight loss measurements (data not shown). The antileukemia effect following anti-CD19 calicheamicin θ immunotoxin therapy was dose-dependent and highly significant in all treatment groups ($p < 0.01$).

Mechanism of Antileukemic Effects Mediated by Anti-CD19 Calicheamicin θ Immunotoxin. The mechanism of antileukemic effects mediated by the anti-CD19 calicheamicin θ immunotoxin was determined on CD19-positive primary ALL blasts and CD19-positive BJAB cells in vitro. We could demonstrate that the anti-CD19 calicheamicin θ immunotoxin induced apoptosis in CD19-positive leukemia cells (Figure 5). Induction of apoptosis by anti-CD19 calicheamicin θ immunotoxin involves processing of caspase 3 as indicated by a decrease in procaspase 3 and increase in 17 kDa active caspase subunit (p17) signals. Interestingly, the level of DNA fragmentation and loss of mitochondria membrane potential was more than 5× higher than that observed with an equivalent amount of free calicheamicin θ (Figure 5B,C), consistent with rapid internalization of the anti-CD19 antibody immunotoxin. The induction of apoptosis was demonstrated to be independent from death-receptor/FADD-mediated signals, since the immunotoxin was as effective in induction of apoptosis parameters in BJAB/FADD-dn cells with dominant negative death receptor domains as in BJAB control cells (Figure 5B,C). Results of control experiments with Fas ligand and anti-CD95 mAb for validation of experiments with BJAB/FADD-dn cells shown here were previously reported (*29*). Importantly, these proapoptotic effects were observed under time and concentration conditions with no effect on cell viability (Figure 5D).

DISCUSSION

In order to solve the problem of poor outcome in relapsed pediatric ALL patients, targeting of CD19 constitutes an appealing approach based on the following considerations. The cell surface glycoprotein of the immunoglobulin superfamily CD19 is absent from hematopoietic stem cells, and in healthy individuals, its presence is exclusively restricted to the B-cell lineage and follicular dendritic cells. Furthermore, CD19 is not shed from the cell surface and is rarely lost during neoplastic transformation (*31*). The antigen is expressed on most B-cell malignancies, including cells from patients with acute lymphoblastic leukemia (ALL) (*32*). Importantly, CD19 is consistently expressed on B-precursor and mature B-ALLs, whereas CD20 is frequently absent on B-precursor ALLs. Furthermore, high levels of CD19 expression remains unchanged as shown in diagnostic and relapse flow cytometry phenotypes in childhood ALL (*33*).

The use of CD19-specific antibody conjugates has been evaluated for immunotherapy of B-lineage malignancies with promising results (*34*−*40*). This also applies to anti-CD19 immunotoxins with idarubicin, ricin A, blocked ricin (dose range 20−50 μg/kg) (*34, 35, 41*), deglycosylated ricin A chain (MTD 16 mg/m^2 = 320 μg/kg) (*36*) and genistein (dose range 100−320 μg/kg) (*37*), which showed efficacy in vivo. Here, we report for the first time construction, effect, and mechanism of a novel anti-CD19 immunotoxin using calicheamicin θ (Figures 1−4). The efficacy over the reported immunotoxins was improved, since a dosage of 10 μg/kg was sufficient to eradicate CD19 leukemia in mice (Figure 4). This is mainly a result of the highly potent calicheamicin θ (Tables 1 and 2), a synthetic derivative of calicheamicin γ.

The use of calicheamicin in the treatment of adult and pediatric B-cell malignancies is well-established (*37, 42, 43*). In fact, calicheamicin γ, which is up to 3 logs less potent than calicheamicin θ {Nicolaou, 1994 174 /id}, is currently used as

the cytotoxic component of an immunotoxin targeting CD33 (gemtuzumab ozogamicin, CMA-676, Mylotarg). Efficacy and tolerability of gemtuzumab ozogamicin has been evaluated in children with relapsed or refractory myeloid leukemia, with a promising response rate of 25% (*42*). An important aspect for the efficacy of the gemtuzumab ozogamicin is rapid internalization and subsequent induction of cell death (*44*). We could also demonstrate rapid internalization of the anti-CD19 antibody used for the calicheamicin θ anti-CD19 immunotoxin (Figure 1). This translated into excellent efficacy and specificity in a xenograft model of CD19-positive leukemia in mice (Figure 4). Specifically, mice treated with 10 μg/kg anti-CD19 calicheamicin θ immunotoxin were free of leukemia in contrast to controls treated with an equivalent dose of a nonspecific control immunotoxin (anti-GD2 calicheamicin θ immunotoxin). This control immunotoxin showed a minor nonspecific antileukemic effect at the highest dose level (10 μg/kg) (Figure 4) most likely due to a prolonged half-life of calicheamicin θ as a result of its conjugation to a monoclonal antibody. Importantly, induction of death receptor independent apoptosis proceeding through the mitochondrial pathway in a caspase 3 dependent mechanism was demonstrated for the anti-CD19 calicheamicin θ immunotoxin (Figure 5). The apoptotic pathways observed with anti-CD19 calicheamicin θ immunotoxin were no different from those delineated for unconjugated calicheamicin θ (*29*). Importantly, these effects were observed at picomolar concentrations and were over 5-fold higher than effects observed with free calicheamicin θ (Figure 5), indicating the important role of internalization in this process. These findings establish proof of concept that targeting of CD19 using a calicheamicin θ immunotoxin may be effective against CD19-positive malignancies. Considering established work with calicheamicin γ immunotoxin (gemtuzumab ozogamicin) and in view of the advantages of calicheamicin θ over calicheamicin γ, this study provides an important baseline for the clinical development of an anti-CD19 calicheamicin θ immunotoxin.

ACKNOWLEDGMENT

We would like to thank Anne Strandsby for excellent technical assistance. This work was supported by the Deutsche Forschungsgemeinschaft, Emmy-Noether Program, Lo 635/2-1 (H.N.L) and Kinderkrebs Neuroblastomforschung e.V. Kinderleben e.V. Berlin (A.P.) and AIP fellowships from the Charité (K.B.).

LITERATURE CITED

(1) Schrappe, M., Reiter, A., Ludwig, W. D., Harbott, J., Zimmermann, M., Hiddemann, W., Niemeyer, C., Henze, G., Feldges, A., Zintl, F., Kornhuber, B., Ritter, J., Welte, K., Gadner, H., and Riehm, H. (2000) Improved outcome in childhood acute lymphoblastic leukemia despite reduced use of anthracyclines and cranial radiotherapy: results of trial ALL-BFM 90. German-Austrian-Swiss ALL-BFM Study Group. *Blood 95*, 3310–3322.

(2) Pui, C. H., Sandlund, J. T., Pei, D., Rivera, G. K., Howard, S. C., Ribeiro, R. C., Rubnitz, J. E., Razzouk, B. I., Hudson, M. M., Cheng, C., Raimondi, S. C., Behm, F. G., Downing, J. R., Relling, M. V., and Evans, W. E. (2003) Results of therapy for acute lymphoblastic leukemia in black and white children. *JAMA 290*, 2001–2007.

(3) Pui, C. H., Relling, M. V., Campana, D., and Evans, W. E. (2002) Childhood acute lymphoblastic leukemia. *Rev. Clin. Exp. Hematol. 6*, 161–180.

(4) Henze, G., Fengler, R., Hartmann, R., Kornhuber, B., Janka-Schaub, G., Niethammer, D., and Riehm, H. (1991) Six-year experience with a comprehensive approach to the treatment of recurrent childhood acute lymphoblastic leukemia (ALL-REZ BFM 85). A relapse study of the BFM group. *Blood 78*, 1166–1172.

(5) Cheson, B. D. (2006) Monoclonal antibody therapy for B-cell malignancies. *Semin. Oncol. 33*, S2–14.

(6) Griffin, T. C., Weitzman, S., Weinstein, H., Chang, M., Cairo, M., Hutchison, R., Shiramizu, B., Wiley, J., Woods, D., Barnich, M., and Gross, T. G. (2009) A study of rituximab and ifosfamide, carboplatin, and etoposide chemotherapy in children with recurrent/refractory B-cell (CD20+) non-Hodgkin lymphoma and mature B-cell acute lymphoblastic leukemia: a report from the Children's Oncology Group. *Pediatr. Blood Cancer 52*, 177–181.

(7) de Vries, M. J., Veerman, A. J., and Zwaan, C. M. (2004) Rituximab in three children with relapsed/refractory B-cell acute lymphoblastic leukaemia/Burkitt non-Hodgkin's lymphoma. *Br. J. Hamaetol. 125*, 414–415.

(8) Thomas, D. A., Faderl, S., O'Brien, S., Bueso-Ramos, C., Cortes, J., Garcia-Manero, G., Giles, F. J., Verstovsek, S., Wierda, W. G., Pierce, S. A., Shan, J., Brandt, M., Hagemeister, F. B., Keating, M. J., Cabanillas, F., and Kantarjian, H. (2006) Chemoimmunotherapy with hyper-CVAD plus rituximab for the treatment of adult Burkitt and Burkitt-type lymphoma or acute lymphoblastic leukemia. *Cancer 106*, 1569–1580.

(9) Gisselbrecht, C. (2008) Use of rituximab in diffuse large B-cell lymphoma in the salvage setting. *Br. J. Hamaetol. 143*, 607–621.

(10) Martin, A., Conde, E., Arnan, M., Canales, M. A., Deben, G., Sancho, J. M., Andreu, R., Salar, A., Garcia-Sanchez, P., Vazquez, L., Nistal, S., Requena, M. J., Donato, E. M., Gonzalez, J. A., Leon, A., Ruiz, C., Grande, C., Gonzalez-Barca, E., and Caballero, M. D. (2008) R-ESHAP as salvage therapy for patients with relapsed or refractory diffuse large B-cell lymphoma: the influence of prior exposure to rituximab on outcome. A GEL/TAMO study. *Haematologica 93*, 1829–1836.

(11) Hilchey, S. P.; Hyrien, O.; Mosmann, T. R.; Livingstone, A. M.; Friedberg, J. W.; Young, F.; Fisher, R. I.; Kelleher; R. J., Jr., Bankert, R. B.; Bernstein, S. H. (2009) Rituximab immunotherapy results in the induction of a lymphoma idiotype-specific T-cell response in patients with follicular lymphoma: support for a "vaccinal effect" of rituximab. *Blood*.

(12) Bonavida, B. (2007) Rituximab-induced inhibition of anti-apoptotic cell survival pathways: implications in chemo/immunoresistance, rituximab unresponsiveness, prognostic and novel therapeutic interventions. *Oncogene 26*, 3629–3636.

(13) Hagenbeek, A., and Lewington, V. (2005) Report of a European consensus workshop to develop recommendations for the optimal use of (90)Y-ibritumomab tiuxetan (Zevalin) in lymphoma. *Ann. Oncol. 16*, 786–792.

(14) Scheuermann, R. H., and Racila, E. (1995) CD19 antigen in leukemia and lymphoma diagnosis and immunotherapy. *Leuk. Lymphoma 18*, 385–397.

(15) Herrera, L., Stanciu-Herrera, C., Morgan, C., Ghetie, V., and Vitetta, E. S. (2006) Anti-CD19 immunotoxin enhances the activity of chemotherapy in severe combined immunodeficient mice with human pre-B acute lymphoblastic leukemia. *Leuk. Lymphoma 47*, 2380–2387.

(16) Gerber, H. P., Kung-Sutherland, M., Stone, I., Morris-Tilden, C., Miyamoto, J., McCormick, R., Alley, S. C., Okeley, N., Hayes, B., Hernandez-Ilizaliturri, F. J., McDonagh, C. F., Carter, P. J., Benjamin, D., Grewal, I. S. (2009) Potent antitumor activity of the anti-CD19 auristatin antibody-drug conjugate hBU12-vcMMAE against rituximab sensitive and resistant lymphomas. *Blood*.

(17) Zein, N., Sinha, A. M., McGahren, W. J., and Ellestad, G. A. (1988) Calicheamicin gamma 1I: an antitumor antibiotic that cleaves double-stranded DNA site specifically. *Science 240*, 1198–1201.

(18) Lee, M. D., Manning, J. K., Williams, D. R., Kuck, N. A., Testa, R. T., and Borders, D. B. (1989) Calicheamicins, a novel family of antitumor antibiotics. 3. Isolation, purification and characterization of calicheamicins beta 1Br, gamma 1Br, alpha 2I, alpha 3I, beta 1I, gamma 1I and delta 1I. *J. Antibiot. 42*, 1070–1087.

(19) Acton, E. M., Tong, G. L., Mosher, C. W., and Wolgemuth, R. L. (1984) Intensely potent morpholinyl anthracyclines. *J. Med. Chem. 27*, 638–645.

(20) Raso, V., Ritz, J., Basala, M., and Schlossman, S. F. (1982) Monoclonal antibody-ricin A chain conjugate selectively cytotoxic for cells bearing the common acute lymphoblastic leukemia antigen. *Cancer Res. 42*, 457–464.

(21) Zein, N., Poncin, M., Nilakantan, R., and Ellestad, G. A. (1989) Calicheamicin gamma 1I and DNA: molecular recognition process responsible for site-specificity [published erratum appears in Science 1989 Jun 9;244(4909):following 1128]. *Science 244*, 697–699.

(22) Nicolaou, K. C., Dai, W. M., Tsay, S. C., Estevez, V. A., and Wrasidlo, W. (1992) Designed enediynes: a new class of DNA-cleaving molecules with potent and selective anticancer activity. *Science 256*, 1172–1178.

(23) Nicolaou, K. C., Li, T., Nakada, M., Hummel, C. W., and Wrasidlo, W. (1994) Calicheamicin θ^{I}_{1}: a rationally designed molecule with extremely potent and selective DNA cleaving properties and apoptosis inducing activity. *Angew. Chem., Int. Ed. Engl. 33*, 183–186.

(24) Lode, H. N., Reisfeld, R. A., Handgretinger, R., Nicolaou, K. C., Gaedicke, G., and Wrasidlo, W. (1998) Targeted therapy with a novel enediyene antibiotic calicheamicin theta(I)1 effectively suppresses growth and dissemination of liver metastases in a syngeneic model of murine neuroblastoma. *Cancer Res. 58*, 2925–2928.

(25) Wieder, T., Essmann, F., Prokop, A., Schmelz, K., Schulze-Osthoff, K., Beyaert, R., Dorken, B., and Daniel, P. T. (2001) Activation of caspase-8 in drug-induced apoptosis of B-lymphoid cells is independent of CD95/Fas receptor-ligand interaction and occurs downstream of caspase-3. *Blood 97*, 1378–1387.

(26) Lode, H. N., Xiang, R., Varki, N. M., Dolman, C. S., Gillies, S. D., and Reisfeld, R. A. (1997) Targeted interleukin-2 therapy for spontaneous neuroblastoma metastases to bone marrow. *J. Natl. Cancer Inst. 89*, 1586–1594.

(27) Scudiero, D. A., Shoemaker, R. H., Paull, K. D., Monks, A., Tierney, S., Nofziger, T. H., Currens, M. J., Seniff, D., and Boyd, M. R. (1988) Evaluation of a soluble tetrazolium/formazan assay for cell growth and drug sensitivity in culture using human and other tumor cell lines. *Cancer Res. 48*, 4827–4833.

(28) Gunther, R., Chelstrom, L. M., Tuel-Ahlgren, L., Simon, J., Myers, D. E., and Uckun, F. M. (1995) Biotherapy for xenografted human central nervous system leukemia in mice with severe combined immunodeficiency using B43 (anti-CD19)-pokeweed antiviral protein immunotoxin. *Blood 85*, 2537–2545.

(29) Prokop, A., Wrasidlo, W., Lode, H., Herold, R., Lang, F., Henze, G., Dorken, B., Wieder, T., and Daniel, P. T. (2003) Induction of apoptosis by enediyne antibiotic calicheamicin thetaII proceeds through a caspase-mediated mitochondrial amplification loop in an entirely Bax-dependent manner. *Oncogene 22*, 9107–9120.

(30) Knoll, K., Wrasidlo, W., Scherberich, J. E., Gaedicke, G., and Fischer, P. (2000) Targeted therapy of experimental renal cell carcinoma with a novel conjugate of monoclonal antibody 138H11 and calicheamicin thetaI1. *Cancer Res. 60*, 6089–6094.

(31) Scheuermann, R. H., and Racila, E. (1995) CD19 antigen in leukemia and lymphoma diagnosis and immunotherapy. *Leuk. Lymphoma 18*, 385–397.

(32) Uckun, F. M., Jaszcz, W., Ambrus, J. L., Fauci, A. S., Gajl-Peczalska, K., Song, C. W., Wick, M. R., Myers, D. E., Waddick, K., and Ledbetter, J. A. (1988) Detailed studies on expression and function of CD19 surface determinant by using B43 monoclonal antibody and the clinical potential of anti-CD19 immunotoxins. *Blood 71*, 13–29.

(33) Borowitz, M. J., Pullen, D. J., Winick, N., Martin, P. L., Bowman, W. P., and Camitta, B. (2005) Comparison of diagnostic and relapse flow cytometry phenotypes in childhood acute lymphoblastic leukemia: implications for residual disease detection: a report from the children's oncology group. *Cytometry B Clin. Cytom. 68*, 18–24.

(34) Grossbard, M. L., Multani, P. S., Freedman, A. S., O'Day, S., Gribben, J. G., Rhuda, C., Neuberg, D., and Nadler, L. M. (1999) A Phase II study of adjuvant therapy with anti-B4-blocked ricin after autologous bone marrow transplantation for patients with relapsed B-cell non-Hodgkin's lymphoma. *Clin. Cancer Res. 5*, 2392–2398.

(35) Grossbard, M. L., Gribben, J. G., Freedman, A. S., Lambert, J. M., Kinsella, J., Rabinowe, S. N., Eliseo, L., Taylor, J. A., Blattler, W. A., and Epstein, C. L. (1993) Adjuvant immunotoxin therapy with anti-B4-blocked ricin after autologous bone marrow transplantation for patients with B-cell non-Hodgkin's lymphoma. *Blood 81*, 2263–2271.

(36) Stone, M. J., Sausville, E. A., Fay, J. W., Headlee, D., Collins, R. H., Figg, W. D., Stetler-Stevenson, M., Jain, V., Jaffe, E. S., Solomon, D., Lush, R. M., Senderowicz, A., Ghetie, V., Schindler, J., Uhr, J. W., and Vitetta, E. S. (1996) A phase I study of bolus versus continuous infusion of the anti-CD19 immunotoxin, IgG-HD37-dgA, in patients with B-cell lymphoma. *Blood 88*, 1188–1197.

(37) Uckun, F. M., Messinger, Y., Chen, C. L., O'Neill, K., Myers, D. E., Goldman, F., Hurvitz, C., Casper, J. T., and Levine, A. (1999) Treatment of therapy-refractory B-lineage acute lymphoblastic leukemia with an apoptosis-inducing CD19-directed tyrosine kinase inhibitor. *Clin. Cancer Res. 5*, 3906–3913.

(38) Chen, C. L., Levine, A., Rao, A., O'Neill, K., Messinger, Y., Myers, D. E., Goldman, F., Hurvitz, C., Casper, J. T., and Uckun, F. M. (1999) Clinical pharmacokinetics of the CD19 receptor-directed tyrosine kinase inhibitor B43-Genistein in patients with B-lineage lymphoid malignancies. *J. Clin. Pharmacol. 39*, 1248–1255.

(39) Messmann, R. A., Vitetta, E. S., Headlee, D., Senderowicz, A. M., Figg, W. D., Schindler, J., Michiel, D. F., Creekmore, S., Steinberg, S. M., Kohler, D., Jaffe, E. S., Stetler-Stevenson, M., Chen, H., Ghetie, V., and Sausville, E. A. (2000) A phase I study of combination therapy with immunotoxins IgG-HD37-deglycosylated ricin A chain (dgA) and IgG-RFB4-dgA (Combotox) in patients with refractory CD19(+), CD22(+) B cell lymphoma. *Clin. Cancer Res. 6*, 1302–1313.

(40) Gekeler, V., Boer, R., Uberall, F., Ise, W., Schubert, C., Utz, I., Hofmann, J., Sanders, K. H., Schachtele, C., Klemm, K., and Grunicke, H. (1996) Effects of the selective bisindolylmaleimide protein kinase C inhibitor GF 109203X on P-glycoprotein-mediated multidrug resistance. *Br. J. Cancer 74*, 897–905.

(41) Szatrowski, T. P., Dodge, R. K., Reynolds, C., Westbrook, C. A., Frankel, S. R., Sklar, J., Stewart, C. C., Hurd, D. D., Kolitz, J. E., Velez-Garcia, E., Stone, R. M., Bloomfield, C. D., Schiffer, C. A., and Larson, R. A. (2003) Lineage specific treatment of adult patients with acute lymphoblastic leukemia in first remission with anti-B4-blocked ricin or high-dose cytarabine: Cancer and Leukemia Group B Study 9311. *Cancer 97*, 1471–1480.

(42) Brethon, B., Auvrignon, A., Galambrun, C., Yakouben, K., Leblanc, T., Bertrand, Y., Leverger, G., and Baruchel, A. (2006) Efficacy and tolerability of gemtuzumab ozogamicin (anti-CD33 monoclonal antibody, CMA-676, Mylotarg) in children with relapsed/refractory myeloid leukemia. *BMC Cancer 6*, 172.

(43) Arceci, R. J., Sande, J., Lange, B., Shannon, K., Franklin, J., Hutchinson, R., Vik, T. A., Flowers, D., Aplenc, R., Berger, M. S., Sherman, M. L., Smith, F. O., Bernstein, I., and Sievers, E. L. (2005) Safety and efficacy of gemtuzumab ozogamicin in pediatric patients with advanced CD33+ acute myeloid leukemia. *Blood 106*, 1183–1188.

(44) van, D. V. V., te Marvelde, J. G., Hoogeveen, P. G., Bernstein, I. D., Houtsmuller, A. B., Berger, M. S., and Van Dongen, J. J. (2001) Targeting of the CD33-calicheamicin immunoconjugate Mylotarg (CMA-676) in acute myeloid leukemia: in vivo and in vitro saturation and internalization by leukemic and normal myeloid cells. *Blood 97*, 3197–3204.

BC900128H